European Geosciences Union (EGU) General Assembly 2025
Date: 27 April 2025 – 2 May 2025, Venue: Vienna, Austria

Possible origin of authigenic to early diagenetic magnetite through 'Dissimilatory Iron Reduction' (DIR) within Late Archean Banded Iron Formation from Chitradurga Schist Belt (CSB), Western Dharwar Craton (WDC), India

Session: SSP3.4 - ***From Deposition to Deep Burial: The role of physical, chemical, and biological processes on diagenesis, minerals, and fluids***

Soumyadeep Bose[1], Arunava Sen[1], Pradip Samanta[2] and Soumik Mukhopadhyay[1]*
[1]Department of Geological Sciences, Jadavpur University, Kolkata, 700032
[2]Department of Geology, University of North Bengal, Darjeeling, 734013
Presenting author: **Soumyadeep Bose** [*soumyadeepb.geology.rs@jadavpuruniversity.in*]

Abstract ID: EGU25-671

CONTENTS

INTRODUCTION AND GENERAL GEOLOGY

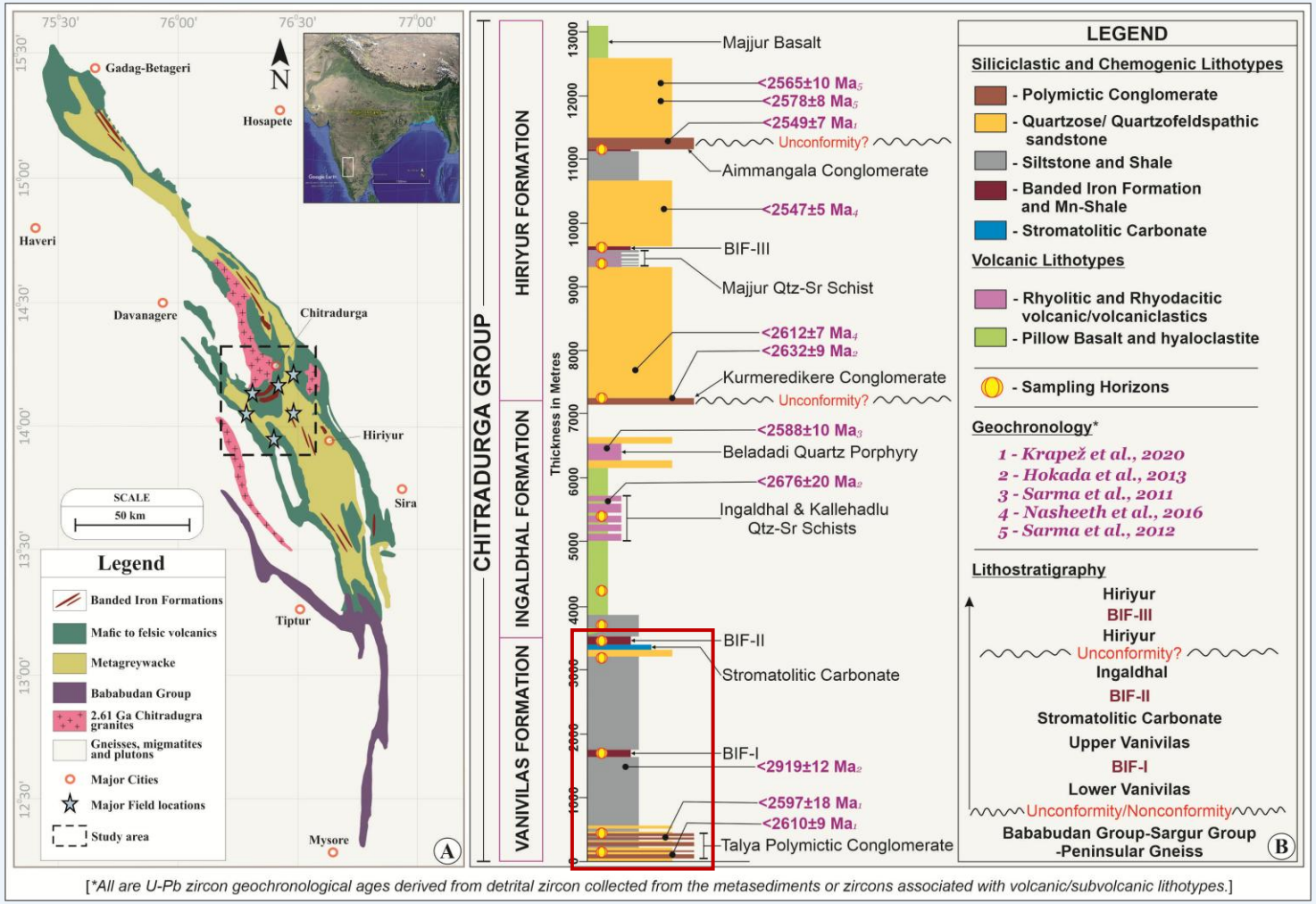

Fig. 1: A) Geological map of Chitradurga Schist Belt (CSB) (modified after Seshadri et al., 1981) (study area marked with black dashed rectangle). Major field locations are marked by blue stars; B) Interpreted Lithostratigraphy of Chitradurga group along with SHRIMP U-Pb Zircon Geochronological data from different lithologies (Krapež et al., 2020 and references therein).

BIFs of VANIVILAS Formation

BIF-I: Shaley BIF

(Chert and Iron rich layers alternating with sulfide bearing greenish Phyllite)

Composition of Iron rich layers: Quartz, Goethite, Magnetite and Chlorite

BIF-II: Cherty BIF

(Chert and Iron rich layers)

Composition of Iron rich layers: Quartz, Hematite, Magnetite, Goethite, Ferrihydrite, Siderite, Greenalite*, Carbonate fluorapatite

***Greenalite $(Fe^{2+},Fe^{3+})_{2-3}Si_2O_5(OH)_4$** can be the key precursors of Archean BIFs, typically found as **nano-crystalline 'lump' like aggregates** within a **chert matrix** along with **oxide, carbonate** and **phosphate** mineral phases separated by a **shrinkage crack network** (Rasmussen et al., 2014a,b; Tosca et al., 2016; Halevy et al., 2017; Rasmussen et al., 2017; Johnson et al., 2018; Rasmussen et al., 2021; Rasmussen et al., 2024).

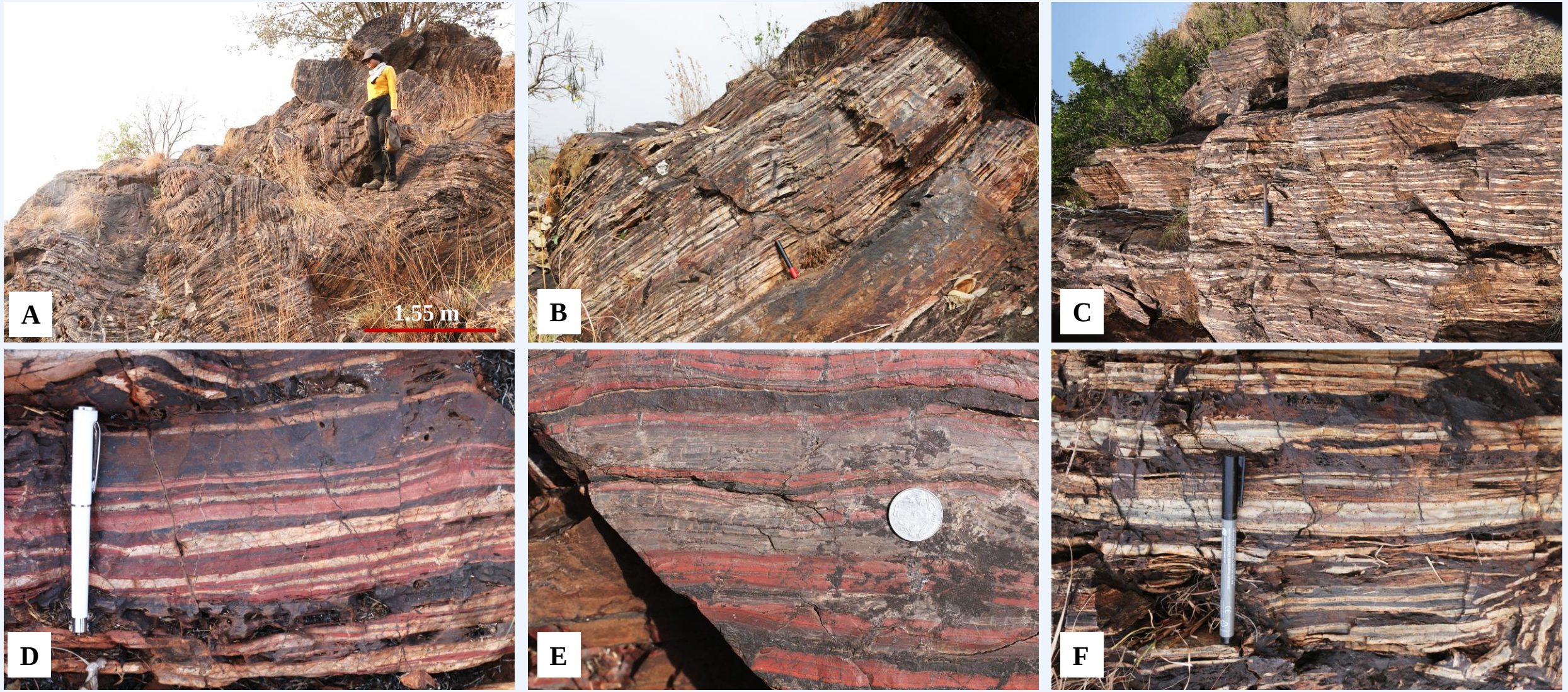

Fig. 2: A), B) & C) Field exposures of the Cherty Banded Iron Formation (BIF-II) near K.M.Kere village, Chitradurga; beds are highly deformed (A) and sub-vertical in nature. Note the presence of centimetre to millimetre scale alternation of chert rich and iron rich layers; D) & E) Field exposures showing the primary beddings defined by jaspillite layers; F) Primary bedding defined by greenish cherty layers. [Scale: Permanent Marker-14cm (B), Geological hammer-30cm (C), Pen-13.5cm (D), Coin diameter- 2.5cm (E), CD Marker-13cm (F)]

PETROGRAPHIC INVESTIGATION AND SEM-EDS ELEMENTAL MAPPING

MICROFACIES OF BIF-II

(1) Red lumpy microfacies (Greenalite + Hematite ± Siderite)
(2) Green lumpy microfacies (Greenalite + Siderite + Apatite ± Magnetite ± Pyrite)
(3) Black lumpy microfacies (Greenalite + Pyrite)

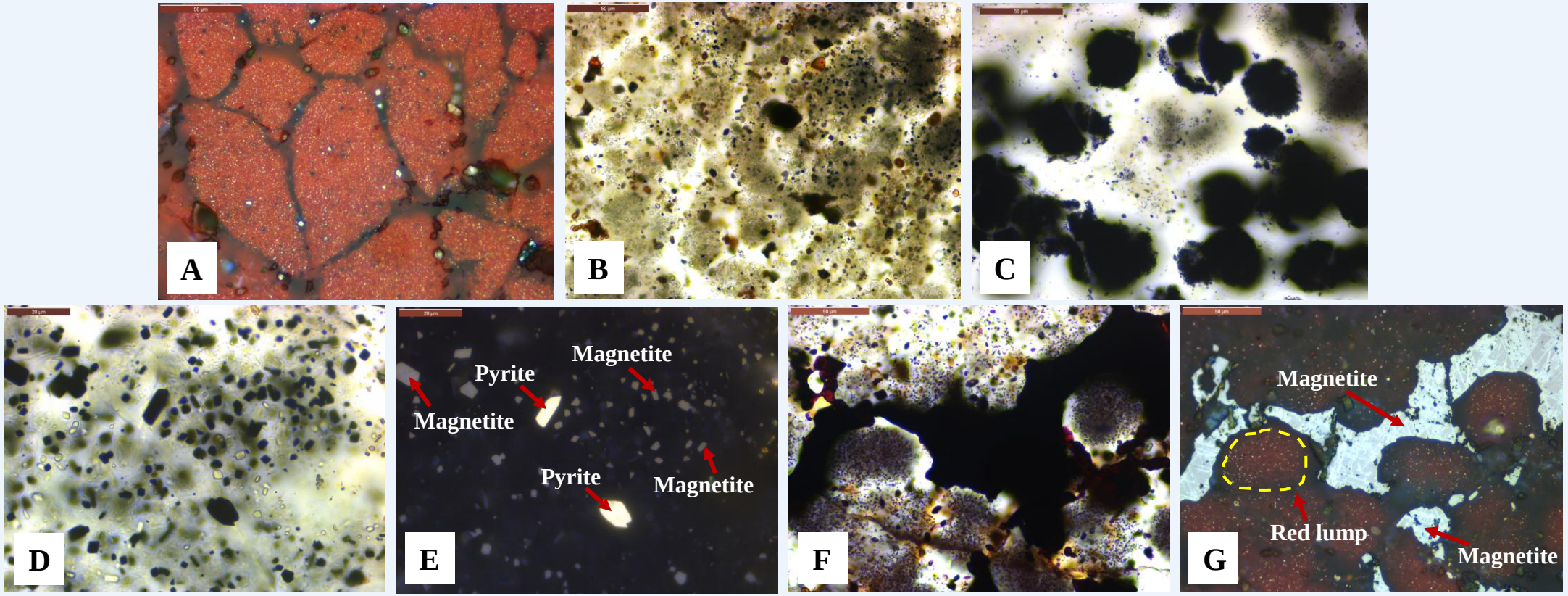

Fig. 3: Petrographic study under polarising microscope reveals the appearance of (A) Red Lumpy microfacies (under reflected light, RL), (B) Green Lumpy microfacies (under plane polarised light, PPL) and (C) Black lumpy microfacies (under plane polarised light, PPL); D) & E) Presence of Magnetite and Pyrite as a lump forming mineral within green lumpy microfacies under PPL and RL respectively; F) & G) Presence of locally developed Magnetite along the periphery of red lumpy microfacies under PPL and RL respectively.

Magnetite within Green lumpy microfacies

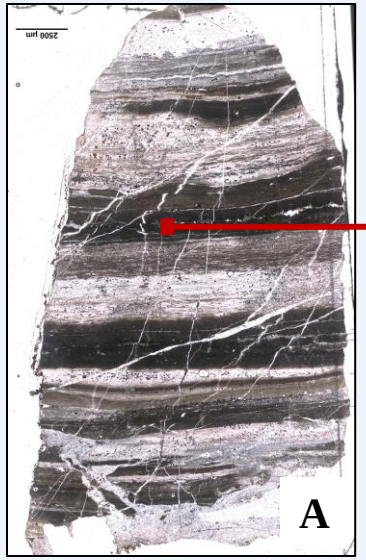

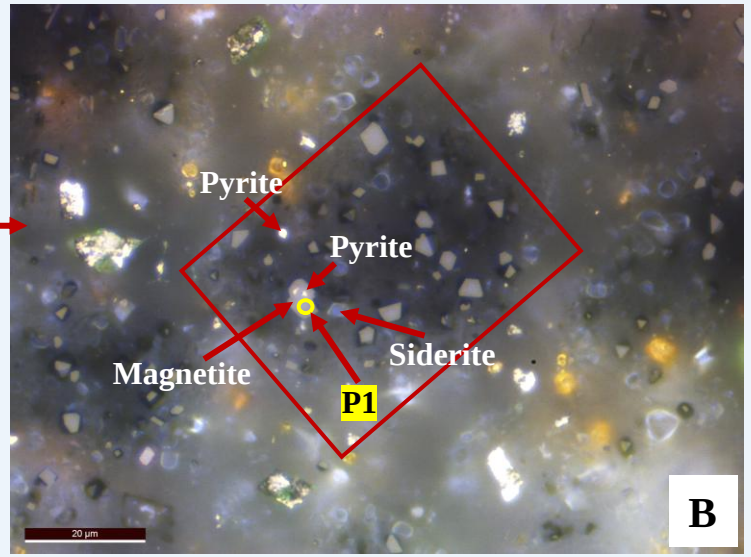

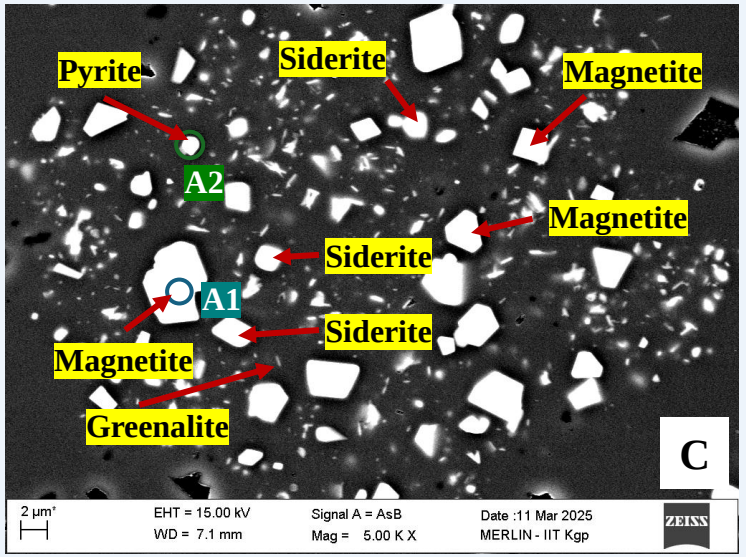

A1	
Element	Weight %
C K	7.64
O K	11.10
MgK	0.53
SiK	1.18
P K	1.50
S K	1.24
CaK	0.33
FeK	74.78
CuK	1.70

A2	
Element	Weight %
C K	10.80
O K	8.77
MgK	0.82
SiK	15.74
P K	1.83
S K	27.47
CaK	0.19
FeK	30.74
CuK	3.64

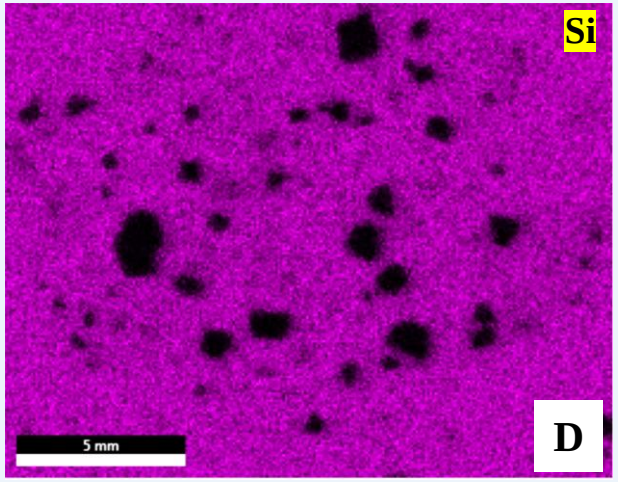

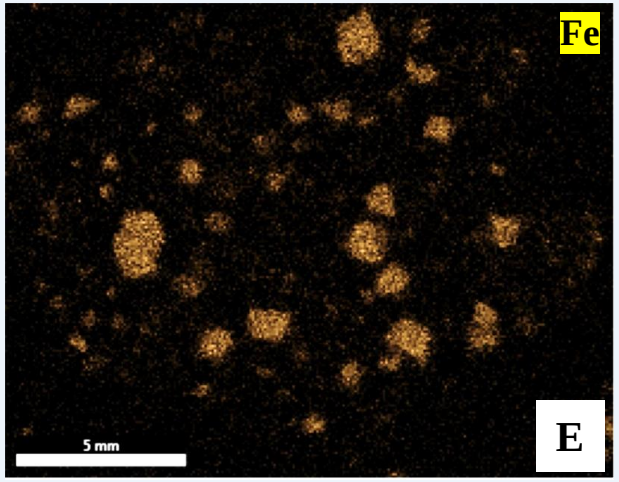

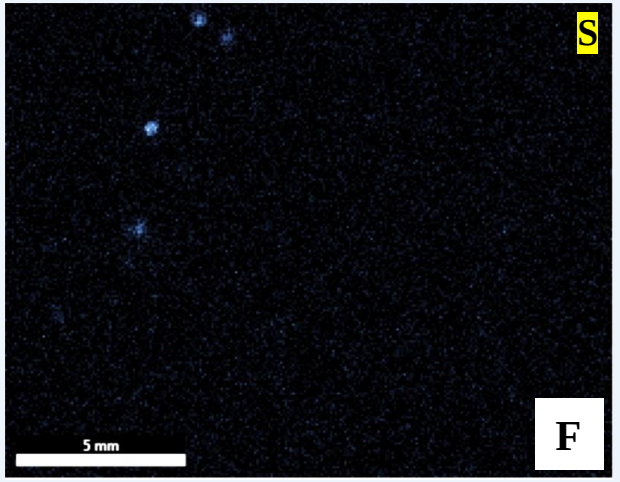

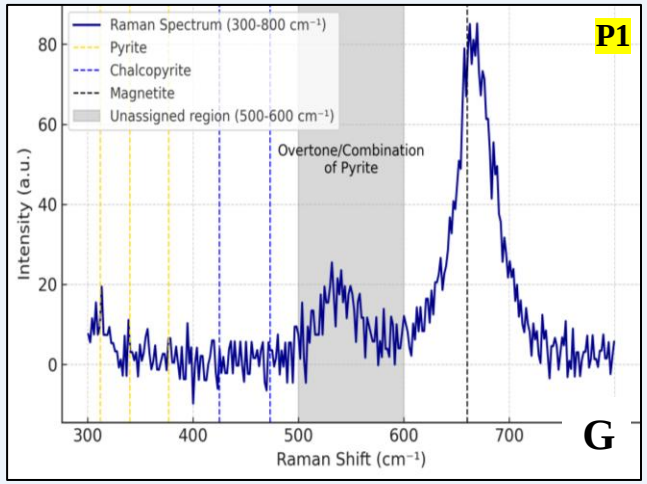

Fig. 4: A) Thin section of studied sample (IG-BIF-11) under PPL; B) enlarged view of the solid rectangle within green lumpy microfacies (4.A) under RL; C) SEM image of the area marked with red hollow rectangle within (4.B), EDS point data for A1 and A2 marked within (4.C); D), E) and F) SEM-EDS elemental mapping of Si, Fe and S respectively for (4.C); G) RAMAN data for the point P1 within (4.B).

Magnetite along the periphery of Red lumpy microfacies

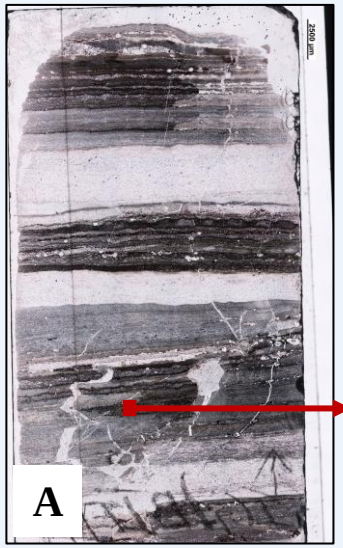

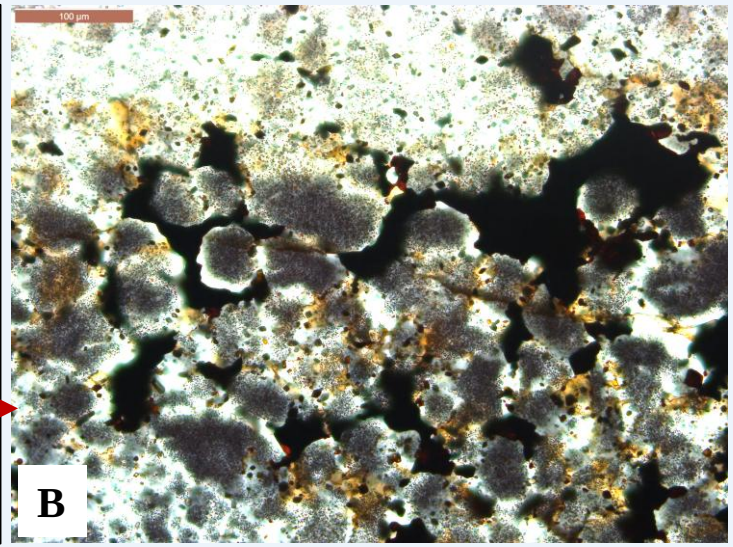

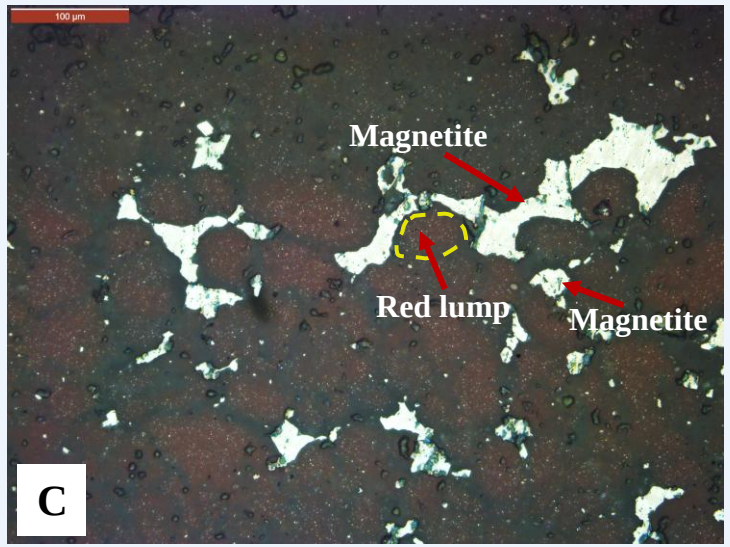

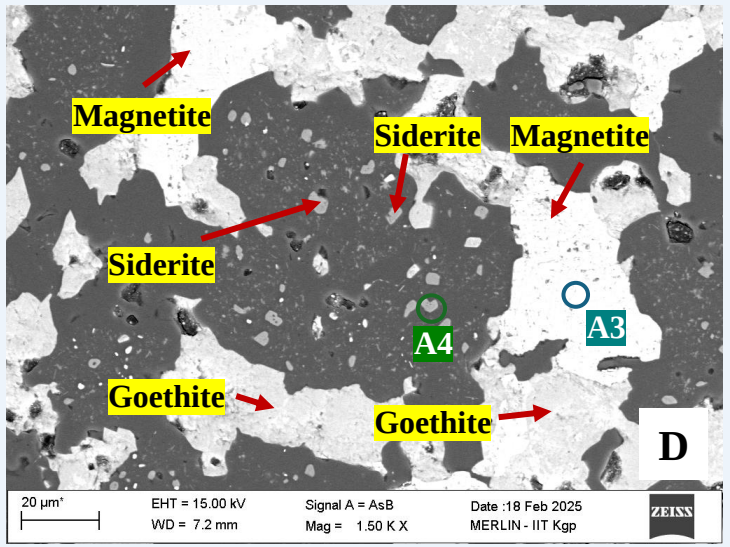

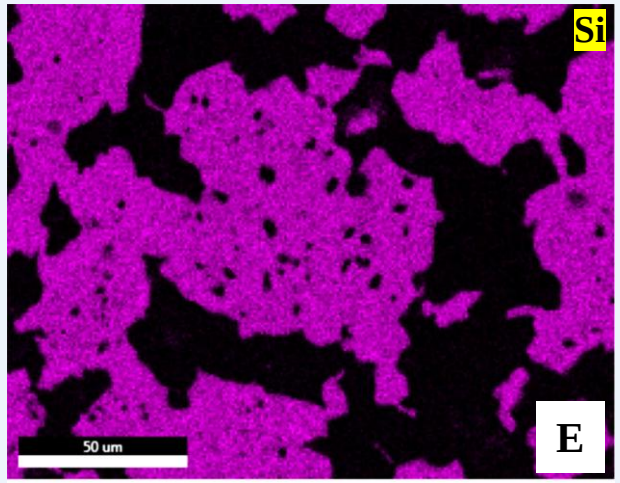

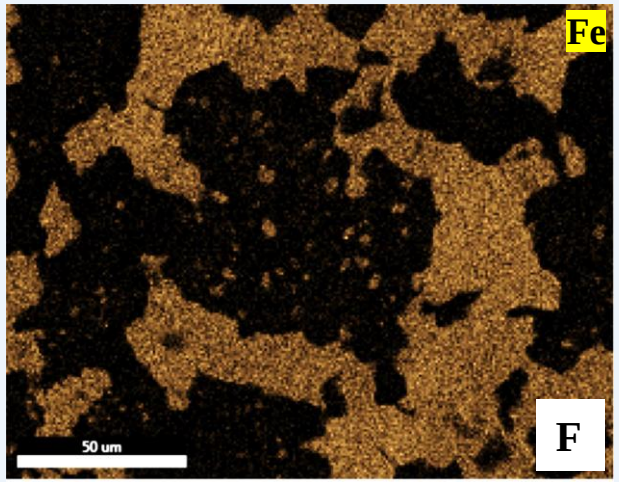

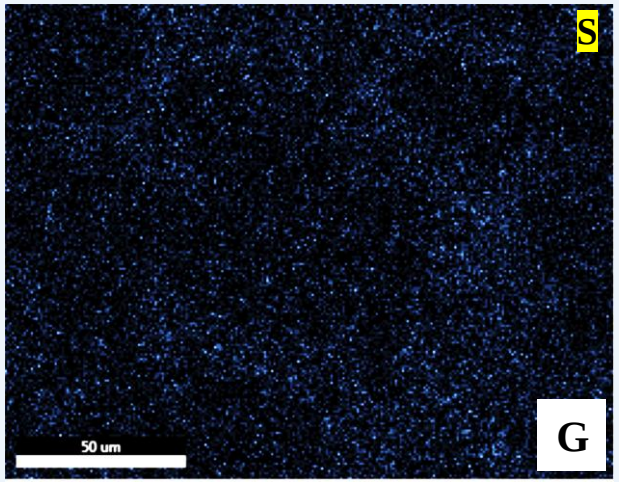

A3	
Element	Weight %
C K	8.56
O K	13.96
MgK	0.47
SiK	2.62
P K	1.46
S K	1.47
CaK	0.49
FeK	70.97

A4	
Element	Weight %
C K	14.50
O K	22.14
MgK	1.14
SiK	7.96
P K	1.11
S K	1.05
CaK	0.17
FeK	51.94

Fig. 5: A) Thin section of studied sample (IG-BIF-2) under PPL; B) & C) enlarged view of the solid rectangle within red lumpy microfacies under PPL and RL respectively; D) SEM image showing anhedral magnetite growing along the periphery of red lumpy microfacies, EDS point data for A3 and A4 marked within (5.D); E), F) and G) SEM-EDS elemental mapping of Si, Fe and S respectively for (5.D).

Magnetite within Black lumpy microfacies

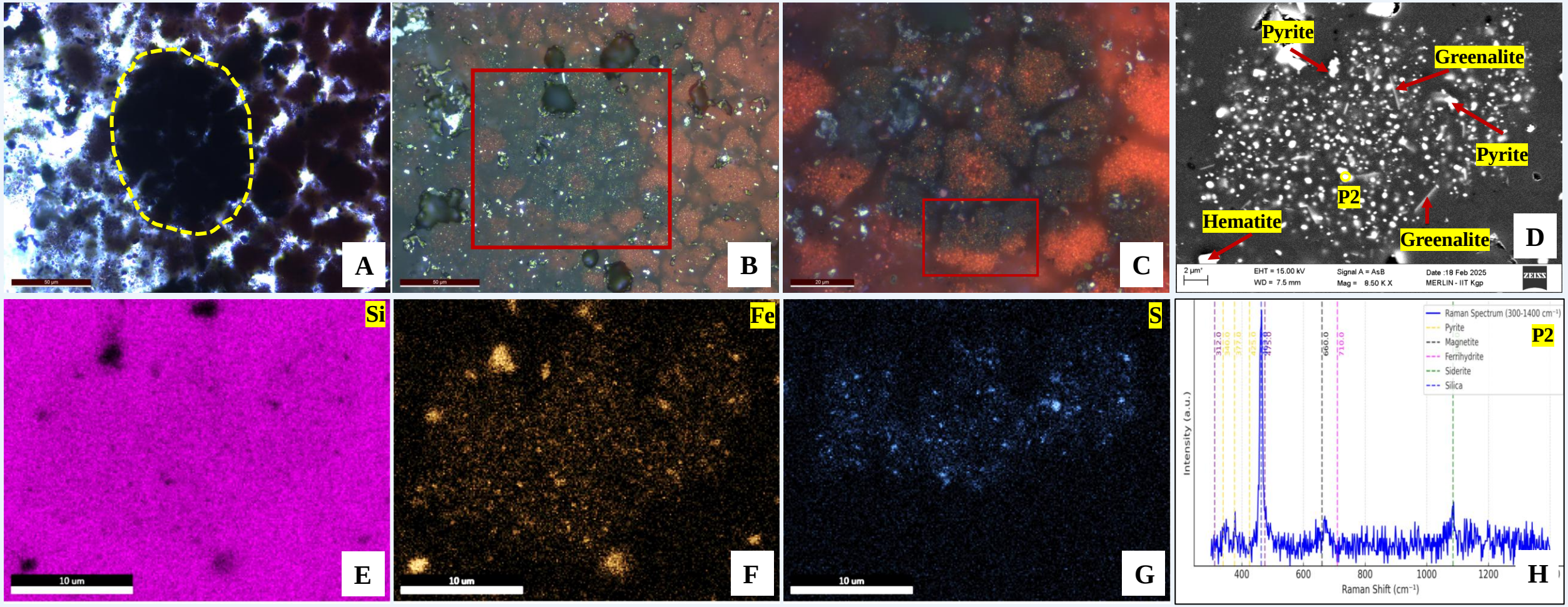

Fig. 6: A) & B) Thin section of studied sample (IG-BIF-1) under PPL and RL respectively. Note the presence of black lumps as clusters of sulfides (yellow dashed outlined) within the jaspillite layer; C) enlarged view of the black lumps marked by hollow red rectangle within (6.B) under RL; D) SEM image of the area marked with red hollow rectangle within (6.C); E), F) & G) SEM-EDS elemental mapping of Si, Fe and S respectively for (6.D); H) RAMAN data for the point P2 within (6.D).

Larger Pyrite grains within Red and Green lumpy microfacies

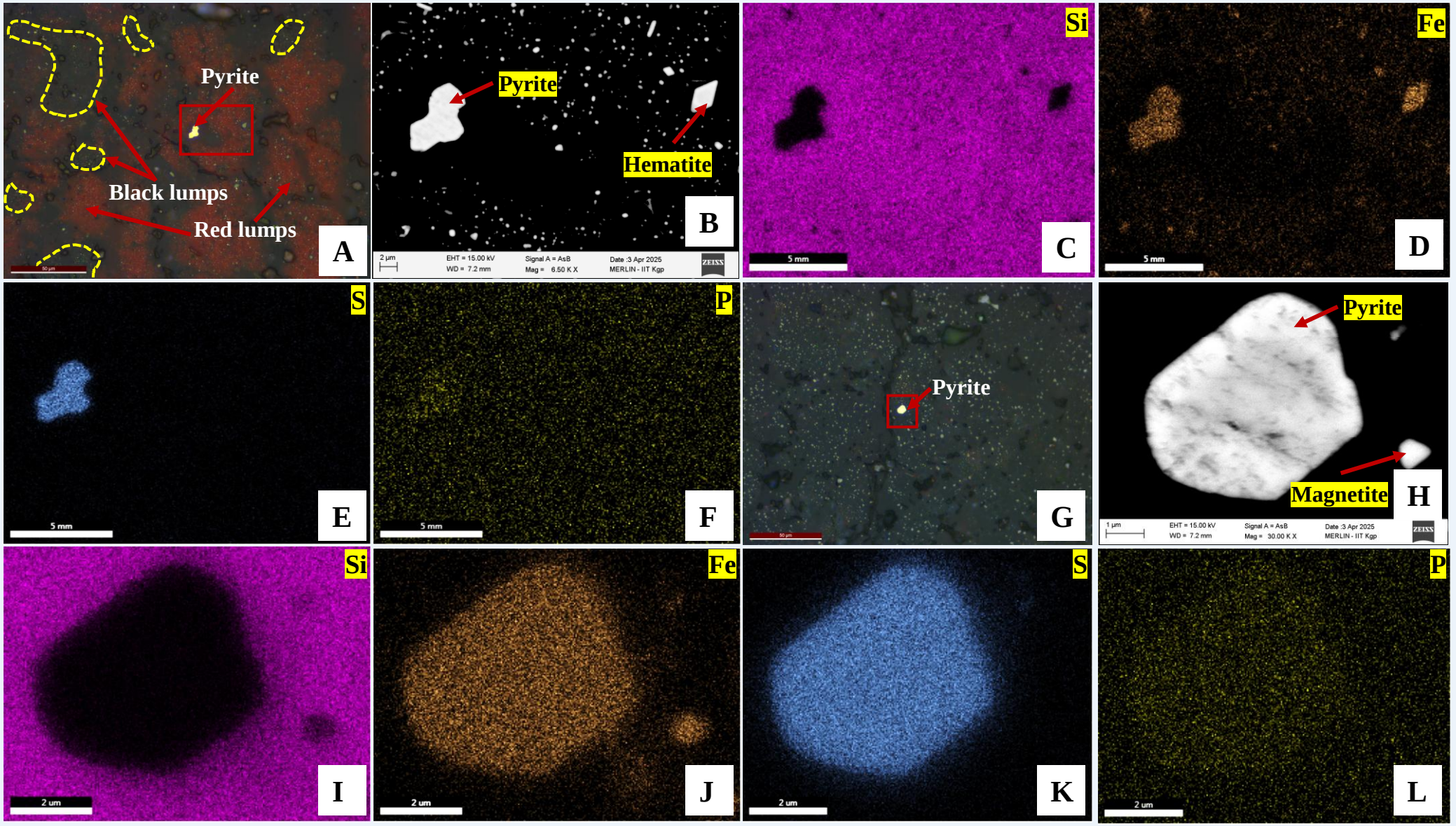

Fig. 7: A) Association of Black lumps as disseminated pockets within Red lumpy microfacies along with a larger variety of pyrite; B) Enlarged view of the area marked by red hollow rectangle within (7.A); C), D), E) & F) SEM-EDS elemental mapping of Si, Fe, S an P respectively for (7.B); G) Large pyrite grain in association with green lumpy microfacies; H) Enlarged view of the area marked by red hollow rectangle within (7.G); I), J), K) & L) SEM-EDS elemental mapping of Si, Fe, S an P respectively for (7.H) [note the enrichment of P within the larger pyrite grains].

DISCUSSION

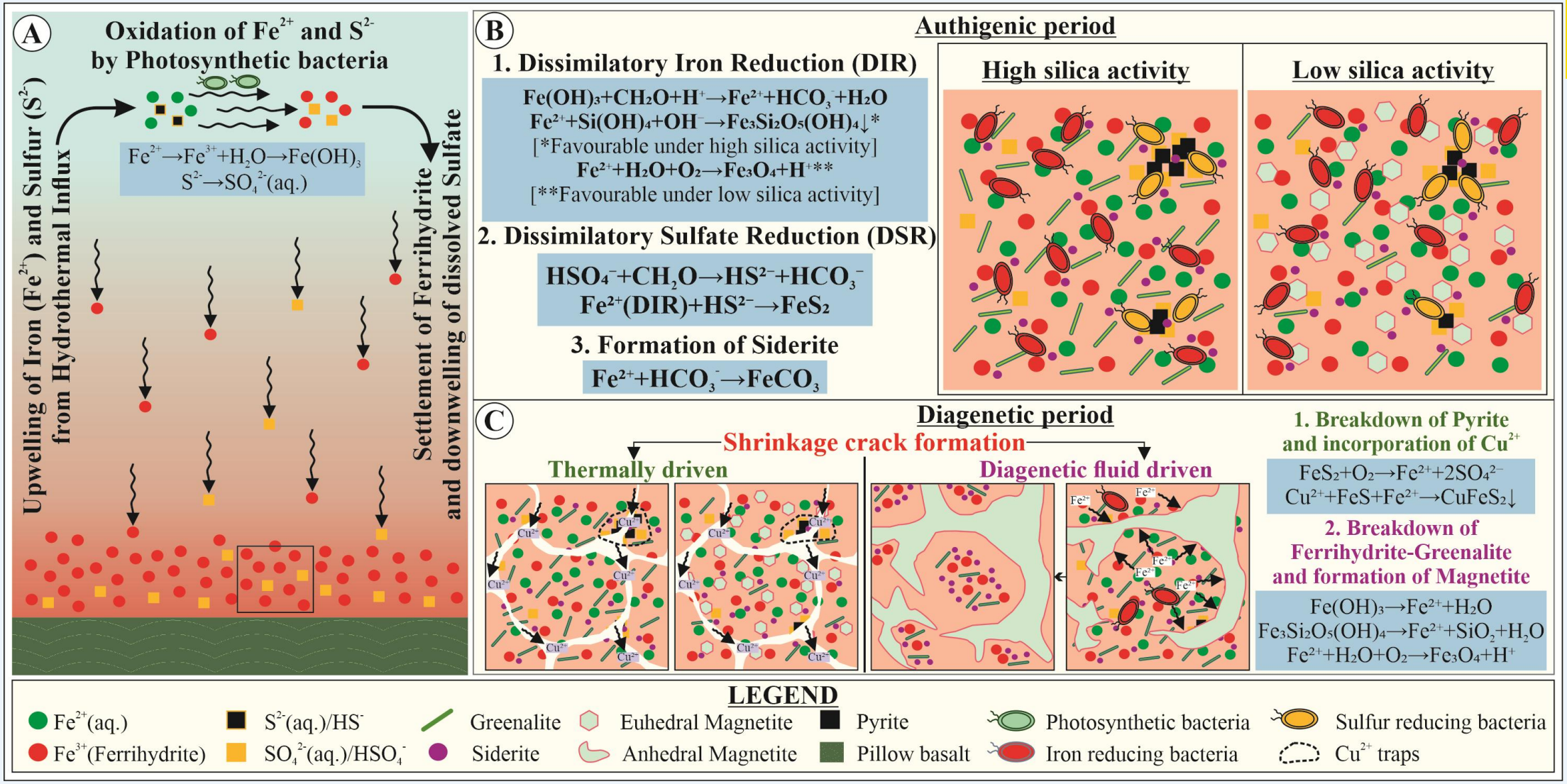

Fig. 8: Schematic diagram for A) Iron (Fe) and Sulfur (S) cycling within Archean ocean; B) & C) role of microbiota during authigenic and early diagenetic stages to form the primordial mineral assemblages along with the effect of different types of shrinkage cracks in modifying the primary precipitates. [Bebie and Schoonen 1999; Rasmussen et al, 2024; Wang et al., 2023 and references therein]

CONCLUSIONS

- The **Late Archean BIF** of the **Chitradurga Schist Belt (CSB)**, particularly within the lowermost **Vanivilas Formation** (BIF-II), preserves primary features with greenalite-rich assemblages in a chert matrix, precipitated from anoxic, hydrothermally influenced seawater and modified by late stage events. Three distinct microfacies have been identified- **red (greenalite + hematite ± siderite), green (greenalite + siderite + apatite ± magnetite/pyrite),** and **black (greenalite + pyrite),** separated by **shrinkage cracks**.

- **Shrinkage cracks** may form due to **diagenetic dehydration of ferrihydrite and greenalite, hydrostatic overpressure, rapid fluid escape**, and, most significantly, **episodic heat influx in a back-arc basin**. Their formation is critical, as it signifies the **termination of active biogeochemical cycles.**

- The formation of **magnetite** within the primary depositional environment associated with these microfacies can be explained in two distinct stages:(1) **Authigenic stage:** Submicron-scale, euhedral magnetite occurs as a lump-forming mineral within green lumpy microfacies, while nanoscale magnetite is found in association with pyrite within black lumpy microfacies; (2) **Early diagenetic stage:** Anhedral magnetite is observed along the periphery of red lumpy microfacies.

- **Iron (Fe)** and **Sulfur (S)** in the Archean ocean were likely part of a **coupled biogeochemical cycle**, primarily sourced from hydrothermal vents and transported upward through upwelling. Upon reaching photic zones, they were oxidized by photosynthetic bacteria to form ferrihydrite and dissolved sulfate, and subsequently settled together on the ocean floor under anoxic conditions.

REFERENCES

- *Bebié, J. and Schoonen, M.A., 1999. Pyrite and phosphate in anoxia and an origin-of-life hypothesis. Earth and Planetary Science Letters, 171(1), pp.1-5.*
- *Halevy, I., Alesker, M., Schuster, E.M., Popovitz-Biro, R. and Feldman, Y., 2017. A key role for green rust in the Precambrian oceans and the genesis of iron formations. Nature Geoscience, 10(2), pp.135-139.*
- *Hokada, T., Horie, K., Satish-Kumar, M., Ueno, Y., Nasheeth, A., Mishima, K. and Shiraishi, K., 2013. An appraisal of Archaean supracrustal sequences in Chitradurga schist belt, western Dharwar Craton, southern India. Precambrian Research, 227, pp.99-119.*
- *Johnson, J.E., Muhling, J.R., Cosmidis, J., Rasmussen, B. and Templeton, A.S., 2018. Low-Fe (III) greenalite was a primary mineral from Neoarchean Oceans. Geophysical Research Letters, 45(7), pp.3182-3192.*
- *Krapež, B., Sarma, D.S., Mohan, M.R., McNaughton, N.J., Rasmussen, B. and Wilde, S.A., 2020. Tectonostratigraphy of the Late Archean Dharwar Supergroup, Dharwar Craton, India: Defining a tectonic history from spatially linked but temporally distinct intracontinental and arc-related basins. Earth-Science Reviews, 201, p.102966.*
- *Nasheeth, A., Okudaira, T., Horie, K., Hokada, T. and Satish-Kumar, M., 2016. U-Pb SHRIMP ages of detrital zircons from Hiriyur Formation in Chitradurga greenstone belt and its implication to the Neoarchean evolution of Dharwar craton, south India. Journal of the Geological Society of India, 87, pp.43-54.*
- *Rasmussen, B., Krapež, B. and Meier, D.B., 2014a. Replacement origin for hematite in 2.5 Ga banded iron formation: Evidence for postdepositional oxidation of iron-bearing minerals. Bulletin, 126(3-4), pp.438-446.*
- *Rasmussen, B., Krapež, B. and Muhling, J.R., 2014b. Hematite replacement of iron-bearing precursor sediments in the 3.46-by-old Marble Bar Chert, Pilbara craton, Australia. Bulletin, 126(9-10), pp.1245-1258.*
- *Rasmussen, B., Muhling, J.R., Suvorova, A. and Krapež, B., 2017. Greenalite precipitation linked to the deposition of banded iron formations downslope from a late Archean carbonate platform. Precambrian Research, 290, pp.49-62.*
- *Rasmussen, B., Muhling, J.R. and Krapež, B., 2021. Greenalite and its role in the genesis of early Precambrian iron formations–A review. Earth-Science Reviews, 217, p.103613.*
- *Rasmussen, B., Muhling, J.R. and Tosca, N.J., 2024. Nanoparticulate apatite and greenalite in oldest, well-preserved hydrothermal vent precipitates. Science Advances, 10(4), p.eadj4789.*
- *Sarma, D.S., Fletcher, I.R., Rasmussen, B., McNaughton, N.J., Ram Mohan, M. and Groves, D.I., 2011. Archean gold mineralisation of the western Dharwar craton, India: 2.52 Ga U-Pb ages of hydrothermal monazite and xenotime in gold deposits. Mineralium Deposita, 46, pp.273-288.*
- *Sarma, D.S., McNaughton, N.J., Belusova, E., Mohan, M.R. and Fletcher, I.R., 2012. Detrital zircon U–Pb ages and Hf-isotope systematics from the Gadag Greenstone Belt: Archean crustal growth in the western Dharwar Craton, India. Gondwana Research, 22(3-4), pp.843-854.*
- *Seshadri, T.S., Chaudhuri, A., Harinadha Babu, P., Chayapathi, N., 1981. Chitradurga belt. In: Swaminath, J., Ramakrishnan, M. (Eds.), Early Precambrian Supracrustals of Southern Karnatka. Geological Survey of India Memoir 112, 163–198.*
- *Tosca, N.J., Guggenheim, S. and Pufahl, P.K., 2016. An authigenic origin for Precambrian greenalite: Implications for iron formation and the chemistry of ancient seawater. Bulletin, 128(3-4), pp.511-530.*
- *Wang, Q., Wang, J., Wang, X., Kumar, N., Pan, Z., Peiffer, S., & Wang, Z. (2023). Transformations of ferrihydrite–extracellular polymeric substance coprecipitates driven by dissolved sulfide: interrelated effects of carbon and sulfur loadings. Environmental Science & Technology, 57(10), pp.4342-4353.*

ACKNOWLEDGEMENT

*I would like to express my sincere gratitude to the **Department of Geological Sciences, Jadavpur University**, and the **Department of Geology, University of North Bengal** for providing a conducive environment and essential facilities that supported this research.*

*I am also thankful to the **DST-INSPIRE** Fellowship scheme of the Government of India for the financial assistance provided during my Ph.D. tenure.*

*Furthermore, I extend my heartfelt appreciation to the **European Geosciences Union General Assembly 2025 (EGU 25),** Vienna, Austria, for offering such an esteemed opportunity to present this work at such a prestigious geoscientific platform.*

Thank You